Molecular Modeling of Phosphonate Molecules onto Barium Sulfate Terraced Surfaces

Franca Jones,*,† William R. Richmond,† and Andrew L. Rohl†,‡

AJ Parker Co-operative Research Centre for Hydrometallurgy, Nanochemistry Research Institute, Curtin University of Technology, GPO Box U1987, Perth WA 6845, Australia, and iVEC, 'The hub of advanced computing in Western Australia', 26 Dick Perry Avenue, Technology Park, Kensington WA 6151, Australia

Received: August 31, 2005; In Final Form: January 25, 2006

The adsorption of phosphonate molecules onto mineral surfaces is of interest due to their use as scale inhibitors. Molecular modeling is an important tool that can aid the fundamental understanding of how these inhibitors operate. This paper presents an empirical molecular mechanics study of the adsorption of a series of straight chain phosphonate molecules onto barium sulfate. It has been found that inhibition can be predicted for this straight chain series of molecules, which differ by the number of phosphonate groups present as well as by the chain length. Even more importantly, the modeling results can predict which faces will be preferred, and this has been verified by scanning and transmission electron microscopy on the resultant barite particles. It has been found that, in general, lattice matching results in the lowest replacement energy for all of the organic molecules investigated. The agreement between the experiment and the model confirms that the dominant mechanism of interaction for the additives on barium sulfate is via the deprotonated phosphonate groups with the barium ions on the surface.

Introduction

Barium sulfate precipitation has historically been an area of scientific investigation for a variety of reasons. First, it is a simple precipitation system in which the substrate does not present problems of polymorphism or formation of various hydrates, so it has been used as a model system for studying precipitation theory.[1] Barium sulfate is also widely encountered as a scale product in many industrial processes,[2−4] so there is an interest in understanding how to control its precipitation in order to mitigate scale formation.

Chemical additives containing phosphonate groups are often used to inhibit the formation of this scale.[5−7] It has been found, for instance, that the ionization of the phosphonate group is important;[8] that is, a deprotonated phosphonate molecule inhibits precipitation more strongly than its protonated form. Also, the greater the number of phosphonate groups, the greater the inhibition of precipitation.[9] While the effectiveness of these additives has been well demonstrated in practice, we are only just beginning to achieve a fundamental understanding of their interaction with barium sulfate surfaces at the atomic level.

Molecular modeling is a useful tool in the pursuit of an atomistic understanding of interactions between surfaces and additive molecules. In particular, it provides a means to determine which organic molecules adsorb and which do not and, for those that adsorb, whether adsorption is preferred on particular faces. Molecular modeling also allows us to investigate whether such preferential adsorption might be experimentally revealed through a change in particle morphology.

Previous molecular modeling of barium sulfate has been conducted using empirical potentials by Allan et al.,[10] and, more recently, by Jang et al.,[11] using molecular dynamics. The former study calculated the surface energies and predicted the morphology in vacuo, while the more recent study was a dynamic investigation that tried to take into consideration the hydration of ions. Jang et al.[11] were able to derive many quantities (from IR band frequencies to the density of the barium sulfate) based on their dynamic investigation, but although the barium sulfate surface energy values found in a vacuum were the same as those of ref 10, the solution results still showed some discrepancy when compared with real samples, which illustrates the importance of always using real experimental results to test a model. It should be stressed, however, that this was a thorough study that clearly showed that different surfaces are stabilized in solution and consequently predicted a different morphology of the particle in solution compared to in vacuo.

The work of the de Leeuw group (examples of which are refs 12 and 13) deals with both organic and inorganic impurities, but on calcite. These studies have tried to correlate the adsorption of impurities on particular faces with inhibition on those faces or to predict the effectiveness of organic molecules as inhibitors, in addition to giving information about the energetics of adsorption and where adsorption is preferred. In general, the modeling results in these studies do not always correlate well with experimental findings or, in some cases, relevant experimental data are lacking. This is because the models are, by necessity, much simpler than the real situation.

For some systems, definitive experimental results are difficult to obtain, so modeling offers an alternative; for example, wetting of the hematite surface has been modeled,[14] although definitive experimental results on whether the proposed mechanism for oxide formation is feasible are still unavailable. Fogg et al.[15] conducted a modeling study incorporating both experimental and modeling results, in which docking of organic impurities on tricalcium aluminate was investigated. The predictions from modeling compared very well with the resultant morphology of the particles found in experiments carried out in the presence of each particular additive.

* Corresponding author. Phone: +618 9266 7677. Fax: +618 9266 4699. E-mail: franca@power.curtin.edu.au.
† Curtin University of Technology.
‡ iVEC.

10.1021/jp054916+ CCC: $33.50
Published on Web 03/18/2006

The most relevant literature to this study, however, is the previous work of Rohl et al.,[16] which investigated the adsorption of a diphosphonate molecule onto the surfaces of barium sulfate. This paper reported that the most energetically favorable sites for the diphosphonate molecule were on the (100), (011), and (010) barite surfaces. Experiments showed that the diphosphonate molecule induced the expression of the (011) face at low concentrations and attacked the [001] zone at high concentrations, an observation that provided general agreement with the modeling. Other researchers[17,18] have suggested lattice matching (or molecular recognition) as the main criterion for the inhibitor molecule to be effective, but the molecular modeling study of Rohl et al.[16] suggested that the interaction was more complex and depended on both the degree of lattice matching and the internal strain energy of the molecule to achieve such a match.

More recently, a combined atomic force microscopy (AFM)/modeling study was conducted,[19] using molecular modeling on the (001) face of barite for both flat terraces and kink sites. No graphical figures of the adsorption configurations were given, so no comment can be made as to the similarity or otherwise to previous findings. One thing that it is important to mention, however, is that there are real and significant differences in the relative adsorption energetics of organic molecules on flat terraces versus kink sites. Generally, inhibitor molecules were found to adsorb at kink sites more strongly than on terraces. It is important to recognize that crystal growth normally does not occur on flat (terraced) surfaces but on kinked and stepped surfaces, so these differences in adsorption energy can be important to interpreting experimental results. AFM was able to correlate adsorption with step velocities, and this adsorption was found to follow Langmuir behavior.

In this study, we have extended the work of Rohl et al.[16] to examine the effect that the number of additive phosphonate groups has on the extent of interaction with the barium sulfate surface. In short, does increasing the number of phosphonate groups favor the molecule−surface interaction? It was also of interest to determine whether modeling could predict the phosphonate's ability to inhibit precipitation by relating the calculated replacement energy to the degree of inhibition. If this were possible, inhibition could be tested more cheaply and quickly on computers than by experiment. To begin with, we have looked at adsorption on terraces (flat surfaces) in order to have a baseline with which later we can compare adsorption at steps and kinks. Barium sulfate precipitation experiments were conducted both in the absence and presence of the phosphonate molecules and the rates of de-supersaturation measured in situ. The particles obtained from these experiments were collected for subsequent analysis. These experimental findings were then compared to the modeling results to determine the applicability of the model.

Experimental Section

The precipitation method consisted of adding Na_2SO_4 (0.5 mL, 0.10 M) to a $BaCl_2$ solution (200.5 mL, 0.249 mM) with mixing at a temperature of 25 °C. Inhibitors were made up as 1000 ppm stock solutions in Milli-Q water. Inhibitor was added to the barium chloride solution prior to commencing the precipitation by the addition of sulfate. The pH for all experiments, unless otherwise stated, was 5.6. Precipitation was monitored in situ using conductivity. The linear section of the drop in conductivity with respect to time was used to calculate a de-supersaturation rate. At the end of a precipitation run, particles were either filtered onto 0.22 μm membranes and washed prior to analysis or allowed to settle onto a glass cover slip (previously washed with ethanol and dried). The glass cover slip was used when little precipitation occurred on the time scale of the experiment (2−3 h). The glass cover slip was placed in the solution and left for 3 days at room temperature and under static conditions.

TABLE 1: Simulation Cell Thickness for the Barium Sulfate Faces Studied (Region I and Region II Values Expressed as the Number of Sulfate Layers)

face	cell thickness (Å) of region I + region II	region I (surface)	region II (bulk)
(001)	49	8	6
(011)	48	14	10
(010)	47	10	8
(101)	61	6	16
(100a)	52	6	8
(100b)	65	6	6
(210)	34	12	8
(211)	41	20	6

Electron Microscopy. Samples for scanning electron microscopy (SEM) were prepared either by placing a portion of filter paper (with barite particles on it) onto a carbon-coated SEM stub or by gently dipping the glass cover slips in water before removing the excess water and attaching them to carbon-coated SEM stubs. The stubs were dried in a desiccator before gold sputtering and viewing with a Philips XL30 scanning electron microscope.

Samples for transmission electron microscopy (TEM) were taken from conductivity runs. The particles were collected by filtration on a 0.22 μm cellulose membrane. A small slice was cut from the filter membrane, placed in a vial with about 5 mL of ethanol, and sonicated to disperse the particles. A drop of this ethanol suspension was then cast onto a conventional carbon-coated copper TEM grid and dried in air. TEM images were recorded on a JEOL 2011 transmission electron microscope operating at 200 kV.

Molecular Modeling Method. All of the molecular modeling used empirically derived potentials.

Barium Sulfate. The parameters for the various potentials describing the interactions within barium sulfate were initially taken from Allan et al.[10] (model 2) and were subsequently refined using GULP[20] to best match the known crystal structures of the isostructural pair of strontium and barium sulfate. These derived potentials are listed in the Supporting Information, section A.

The MARVIN code[21] was used to minimize the energy of the surface structures. The program uses a simulation cell, which is split into two regions. Region I contains the surface atoms, and these are allowed to relax, while region II contains sufficient atoms to reproduce the effect of the bulk properties on region I and remains fixed. Thus, region I represents the surface, while region II represents the bulk. The thickness of region II is determined by allowing it to be sufficiently large that the interaction of the bottom-most bulk atoms with the surface atoms is negligible. The thickness of region I on the other hand is determined by that thickness which allows the surface energy (see eq 1) to converge. The thicknesses of the regions, in terms of the number of sulfate layers, are given in Table 1. GULP has recently been extended to surfaces and has access to the rational functional optimization (RFO) minimizer, which is superior to the MARVIN minimizer, as it avoids saddle points. This new method of finding the minimum resulted in lower surface energies for the (001) and (210) surfaces. For all other surfaces, the results are equivalent to the MARVIN values within numerical error. Thus, for the (001) and (210) surfaces, docking of the additives was run using both GULP and MARVIN to

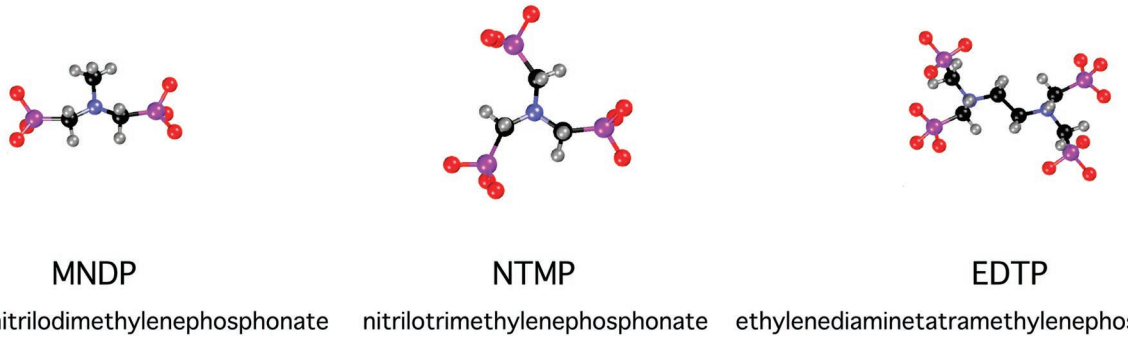

Figure 1. Structures, abbreviations, and full names of the additives investigated in this work (red, oxygen; blue, nitrogen; black, carbon; purple, phosphorus; gray, hydrogen).

ensure the lowest energy configuration was obtained. Interestingly, while the two methods gave different bare surface energies, the minimum energy configurations with docked additives were found to be equivalent using both methods.

The next stage in the simulation is to calculate the expected morphology of barium sulfate using these potentials. There are several approaches one can take, one of which is to define the surface energy as the difference in energy of the surface ions compared to the bulk per unit surface area (eq 1).

$$E_{\text{surf}} = (E_{\text{reg1}} - nE_{\text{bulk}})/A \quad (1)$$

where the E_{reg1} is the energy of region I, n is the number of unit cells in region I, E_{bulk} is the bulk energy of the unit cell, and A is the simulation cell area. Lower surface energies tend to result in more important morphological faces. The morphology obtained in this manner is defined as the "equilibrium" morphology.[21]

Another way of calculating the morphology is to find the energy of attaching another slice of the crystal of depth d_{hkl} to the chosen surface. The smaller the so-called attachment energy, the more important the face is to the morphology of the particle. This results in the "growth" morphology.[21]

Each face can be cut along various planes, producing different surface terminations, and all must be minimized to find the termination with the lowest surface energies for each face. To be sure of finding the most important morphological faces, the 15 faces with the smallest interplanar spacings were chosen and the lowest energy slices for the various faces determined. These faces were then allowed to relax, and a morphology was generated via the Wulff plot[22] using GDIS.[23]

Additives. The organic molecular ions investigated in this work are shown in Figure 1 along with their respective abbreviations.

Due to the complex nature of their protonation states, which involves the formation of zwitterions,[24] all calculations used the fully ionized molecules. This has the drawback that it does not investigate the possible interaction of the protonated nitrogen with the surface, but given that the dominant interaction is expected to be with the phosphonate groups, this is a worthwhile first approximation. The ionization state of the additive is, of course, pH dependent. For EDTP and NTMP, the assumption is essentially true, since the phosphonate groups are almost completely deprotonated at the experimental pH of ~6.[25] However, it has been found in another system that the speciation of a molecule adsorbed to a surface can be different to its speciation in solution.[26] Thus, until there is clear evidence of the protonation state of the adsorbed species at different pHs, it is not possible to determine which species is preferred for adsorption. In this sense, taking the fully deprotonated species is a good means for comparing the additives at their full "inhibiting" potential.

As a comparison to the work of Rohl et al.,[16] the molecule propane-1,3-diphosphonate was also investigated. This molecule is similar to MNDP except that the central atom is carbon rather than nitrogen and it does not contain a methyl group.

The potentials and parameters for these molecules are those derived by Wilson[27] and are essentially a refinement of those reported by Rohl et al.[16] Briefly, these potentials were derived from CVFF in InsightII,[28] while the ESP derived charges were obtained from a Spartan[29] optimization using the PM3 Hamiltonian.[30] Potentials were also required for the interatomic interaction of these molecules with the barium sulfate surface, and these were obtained from the ESFF force field.[31] All of the potential types and the parameters used are listed in the Supporting Information, sections B and C. It should be noted that ref 16 used the CVFF force field to describe most of these interatomic interactions, but the ESFF force field uses the Lennard Jones 9-6 potential rather than the Lennard Jones 12-6 potential.

Docking of the additive is performed by removing the required number of sulfate molecules from the surface (to maintain a charge neutral system) and then placing the phosphonate molecule at a distance from the surface (~2 Å). Due to the periodic boundary nature of both GULP and MARVIN, a charged surface would result in an infinite dipole moment, which is unrealistic; thus, charge neutral systems are investigated. The molecule is then allowed to dock into the surface wherever the energy is lowest. It should also be noted that previous calculations[16] were conducted on much smaller simulation cells (due to computer limitations at the time) and the mode of minimization involved fixing the surface and docking the molecule before the whole system was allowed to relax. With improvements in computer speeds and codes, we have now been able to evaluate several different means of attempting to obtain the global minimum. For all of the additives studied, various starting configurations and sulfate vacancies were investigated. As an added measure, optimizations were conducted whereby the additive was docked while region I was fixed and then the whole was allowed to relax (as done in ref 16) as well as allowing the additives to dock while region I was allowed to relax simultaneously.

Solvation Energies. Solvation energies for the additives were calculated using molecular dynamics as per ref 16 where the additive is surrounded by a sphere of water 20 Å thick, and after thermal equilibration of 1000 steps, the dynamic simulation is undertaken for 10 000 steps. The dynamic simulation is then repeated without the additive at the center, and the solvation

TABLE 2: Calculated and Experimental Lattice Constants (Å) for Strontium and Barium Sulfate

	barium sulfate		strontium sulfate	
	calculated (% difference)	experimental[32]	calculated (% difference)	experimental[33]
a	8.95 (0.79)	8.88	8.39 (0.36)	8.36
b	5.45 (−0.18)	5.46	5.38 (0.56)	5.35
c	7.15 (−0.14)	7.16	6.84 (−0.29)	6.86
vol	346.1 (0.23)	346.9	308.6 (0.59)	306.8

TABLE 3: Elastic Constants, C_{ij} (GPa), Bulk Modulus, *B* (GPa), Compressibility, *X* (GPa^{-1}), and Density, ρ (g cm^{-3}), of Barium Sulfate

	Haussühl[34]	this work
C_{11}	95.15	99.47
C_{12}	51.32	44.47
C_{13}	33.62	30.25
C_{22}	83.66	85.52
C_{23}	32.76	28.87
C_{33}	110.61	114.90
B	58.32	56.01
X	0.0172	0.0178[a]
ρ	4.474[b]	4.440

[a] Calculated from the GULP output according to eq 7b from Jang et al.[11] [b] This value is from Dove and Czank[35] and Hill.[36]

energy is calculated by subtracting the final energy with additive and without additive present. Note that hydration of the adsorbed additive was not considered. The following solvation energies were used:

	solvation energy (kJ mol^{-1})
SO_4^{2-}	−1019[a]
propane-1,3-diphosphonate	−2734[a]
MNDP	−3191
NTMP	−5942
EDTP	−7972

[a] Taken directly from ref 16.

Adsorbed Configurations. There are a large number of adsorbed configurations of the various phosphonate additives shown in this paper. To clearly define the organic molecule against the lattice, most diagrams do not differentiate the phosphonate groups or individual nitrogen atoms, for example, but simply show the whole additive molecule in black and the barium sulfate lattice in gray. Where further insight can be obtained by a more detailed diagram, this is displayed.

Results

The calculated barium and strontium sulfate lattice parameters as determined from the modeling are compared with the experimental values in Table 2. The potential parameters are obviously of high quality, as they are able to reproduce all cell parameters and the cell volumes to well within 1%. Additionally, the elastic constants, bulk modulus, compressibility, and density of barium sulfate calculated with these potentials are compared to literature values in Table 3 and also show a very good match. The calculated surface and attachment energies are listed in Table 4 both with and without relaxation for the 10 faces with the lowest energies.

Before beginning a discussion about the predicted morphology, it is important to describe the two terminations of the (100) face. The *b* face is the termination of the (100) surface with rows of barium atoms and sulfate ions, while the *a* face has alternate barium and sulfate rows missing. Both terminations

TABLE 4: Surface and Attachment Energies for the Lowest 10 Unrelaxed and Relaxed Barium Sulfate Surfaces

	unrelaxed		relaxed	
face	surface (J m^{-2})	attachment (kJ mol^{-1})	surface (J m^{-2})	attachment (kJ mol^{-1})
(001)	0.641	−191.0	0.553	−180.4
(210)	0.705	−218.0	0.524	−208.4
(211)	0.836	−307.8	0.652	−306.8
(010)	0.944	−423.5	0.765	−388.8
(212)	1.01	−439.9	0.763	−452.5
(101)	1.09	−214.2	0.786	−198.7
(311)	1.18	−533.5	0.781	−566.3
(100a)	1.39	−308.7	0.869	−276.9
(100b)	1.29	−300.0	0.875	−254.7
(011)	1.57	−353.1	0.954	−319.3

have similar surface and attachment energies prior to relaxation, and there is already literature suggesting that both terminations are possible growth surfaces for the (100) face.[37] However, after relaxation, the termination with the lowest energy is different for each of the two methods we have employed: the *a* face is lower in the surface energy calculation, while the *b* face is lower in the attachment energy calculation. Since the energies are close and since no particular termination is clearly favored, both faces were investigated. Previous work[16] showed that the *b* face was predicted to be more stable, and as such, the favored adsorption on the *a* face was discounted, as it was not believed that this surface configuration would be exposed in a growing crystal. As a consequence of the results shown here and in light of the above earlier report,[37] it is clear that the (100a) termination should not be discounted on this basis.

For the equilibrium morphology, the following surfaces were found to be present and are listed according to surface energy: (210) < (001) < (211) < (010) < (101). For the growth morphology, the following surfaces were found and are listed according to their attachment energies: (001) < (101) < (210) < (011). Since neither the (212) face nor the (311) face was observed in either morphology, these faces were not further investigated. Of the eight faces left, those important to the morphology depend on which model (growth or equilibrium) one chooses for the morphology calculation. According to the literature data on the most commonly observed faces, the ordering is (001) < (210) < (010) < (100).[11] The results of Allan et al.[10] were based on two potential models used to calculate the surface energies. For model 1, the relaxed surface energies were found to be in the order (001) < (210) < (101) < (211) < (010) < (100) = (011). For model 2, the relaxed surface energies were in the order (210) < (001) < (211) < (101) < (010) < (100) < (011). The order of the relaxed surface energies in the current study did not change significantly on relaxation and is only slightly different from those found by Allan et al.[10] using either potential model, nor is the calculated morphology dramatically different.

The predicted equilibrium (Figure 2a) and growth (Figure 2c) morphologies (from GDIS) using the current potentials are shown in Figure 2. The equilibrium morphology (Figure 2a) is very similar to that reported by Allan et al.[10] using model 2. The morphology most similar to experimental crystals is that obtained from the surface energy (equilibrium morphology) calculations, and this is illustrated by the SEM micrographs of particles grown at low supersaturation in our laboratory (see Figure 2b). It confirms that the equilibrium morphology is the best predictor of morphology for crystals grown slowly under near-equilibrium conditions. The conditions used here consisted of a supersaturation ratio of ~7, temperature of 25 °C, a low

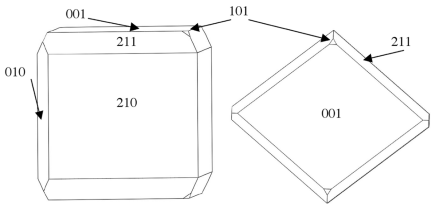

a) Relaxed 'equilibrium' morphology of barium sulfate

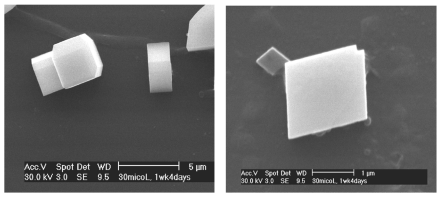

b) Experimentally precipitated barite crystal (SEM micrograph) showing chamfered faces and rhombohedral shape

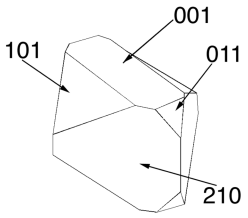

c) Relaxed 'growth' morphology obtained for barium sulfate

Figure 2. (a) Equilibrium and (c) growth morphology obtained for barium sulfate from molecular modeling and (b) SEM micrographs of experimentally precipitated barite crystals ($S \sim 7$).

TABLE 5: Replacement Energies (kJ mol^{-1}) for the Phosphonate Containing Molecules versus the Face on Which They Are Adsorbed (with Solvation Energy Taken into Account)

face	propane-1,3-diphosphonate	MNDP	NTMP	EDTP
(001)	−806.37	−610.53	−1011.80	−2077.04
(210)	−780.99	−533.25	−991.95	−2077.08
(211)	−809.57	−615.00	−1184.57	−1781.81
(010)	−878.80	−686.44	−1149.29	−1989.40
(011)	−985.89	−818.14	−1364.84	−1906.02
(101)	−751.16	−674.02	−1256.13	−2071.72
(100b)	−767.04	−460.16	−1037.54	−2196.25
(100a)	−1066.96	−921.11	−1486.92	−2405.19

pH which promotes the rhombohedral shape,[38] and an aging period between 1 and 2 weeks.

The interaction between the molecule and surface is calculated via the replacement energy:[16]

$$\Delta E_r = (E_{surf+additive} + n\{E_{sulf} + E_{solvSO_4}\}) - (E_{surf} + \{E_{additive} + E_{solvAdd}\}) \quad (2)$$

$E_{surf+additive}$ is the energy of the system with the additive adsorbed, n is the number of sulfates removed from the surface in order to adsorb the additive, E_{sulf} is the energy of the isolated sulfate ion, E_{solvSO_4} is the corresponding solvation energy of the sulfate, E_{surf} is the energy of the surface with the sulfate molecules still in the lattice, $E_{additive}$ is the energy of the free additive, and $E_{solvAdd}$ is the corresponding solvation energy of the additive. In Table 5, the replacement energies for all of the organic molecules on each of the eight faces investigated are shown; the more negative (lower) the replacement energy, the more favorable the interaction of the organic additive with the surface in question.

It is important to recognize that the additive solvation energies play an important role in the determination of the replacement energies. Changes in the solvation energies will change the replacement energy; specifically, the more negative the additive solvation energy, the more positive the replacement energy will become according to eq 2. In this paper, as a first approximation, we have also neglected the solvation of the surface or the solvation of the additive docked on the surface. Thus, it must be kept in mind that solvation has not been completely addressed in this work.

We begin by comparing the results from this study with those of Rohl et al.,[16] for the propane-1,3-diphosphonate molecule. As discussed previously, the use of different interatomic potentials results in different replacement energies being calculated. In this work, the replacement energies are more negative than those previously calculated: $\sim -(1100-700)$ kJ mol^{-1} compared with $\sim -(300-100)$ kJ mol^{-1}.[16] For most of the interatomic potentials, at distances that are indicative of interatomic interactions, the values of the potentials are essentially equivalent, although the attractive interaction between barium ions and additive oxygen atoms is more significant in this work. A comparison of the potential energy curves obtained for this interaction in both studies is shown in Figure 3. The Coulombic terms have not been included here, since both studies used the same charge values for the ions and atoms and thus the Coulombic terms are equivalent. In the work of Rohl et al.,[16] a Buckingham type potential was used for this interaction (the Ba^{2+} ion with the phosphonic oxygen atom) as opposed to the current Lennard Jones 9-6 potential. As can be seen in Figure 3, the interatomic interaction is more negative (attractive) in this study due to the smaller repulsive term.

However, if we compare the order of the replacement energies from both studies, then it becomes clear that the new potentials

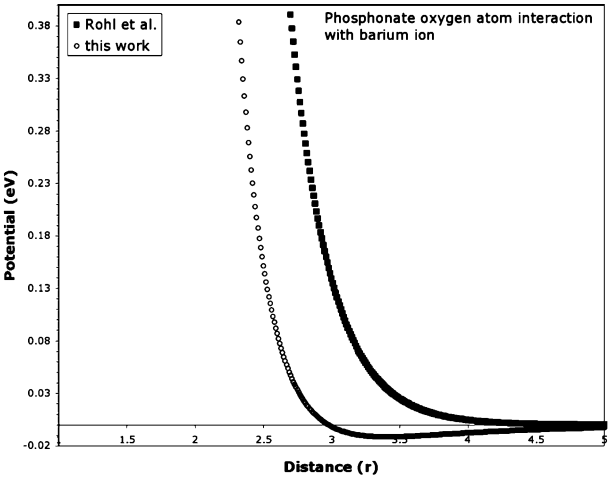

Figure 3. Potential energy curves for the interaction of a barium ion with an oxygen atom from a phosphonate molecule using the CVFF potentials as per ref 16 or the ESFF potential as in this work.

have only slightly affected the relative energetics of the system. The order in the replacement energies is as follows:

This work: (100a) > (011) > (010) > (211) > (001) > (210) > (100b) > (101)

Rohl et al.:[16] (100a) > (011) > (010) > (001) > (100b) > (210) > (211) > (101)

It can be seen from the above comparison that the three most energetically favored faces are the same in each case, with the significant differences being that the (210) and (211) faces are more energetically favored than in ref 16. However, even in ref 16, the binding energy of the organic molecule to the (210) face was found to be greater than that on the (011) face but the internal strain energy of the molecule to accommodate itself on this face made it less energetically favorable. In this work, the greater barium ion to phosphonate oxygen atom interaction appears to have compensated for this to some degree despite the lower bare surface energy found by GULP. If, however, the MARVIN minimized surface energies are used, the order of replacement energies becomes the following:

(100a) > (011) > (210) > (010) > (001) > (211) > (100b) > (101)

Thus, it is clear that both the (210) and (001) faces have slightly more positive replacement energies because of the lower bare surface energies found in GULP.

The adsorbed configurations for all of the faces investigated are shown in Figure 4. The images are shown in side view in order to clearly show whether any "lattice matching" or "molecular recognition" is occurring. As can be seen in Figure 4, the phosphonate groups on the additive do indeed sit mainly in the positions where the sulfate positions (grey crosses) are also found. In the work of Rohl et al.,[16] there were two (100b) configurations that were low in replacement energy, and these configurations differed by only 10 kJ mol^{-1}. The lowest replacement energy, however, was observed for that which had only one phosphonate group docked. In the current work too, both configurations were observed, but in this case, the lowest replacement energy was calculated for the one with both phosphonate groups in the surface (shown in Figure 4e). The replacement energy for this configuration was 31.9 kJ mol^{-1} lower than the case in which only one phosphonate group was

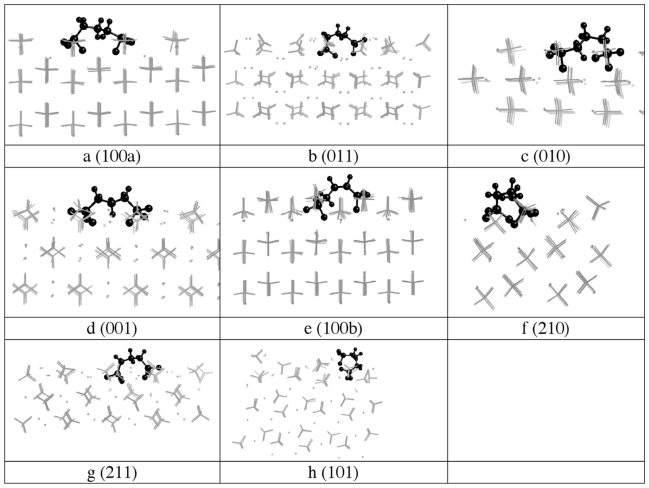

Figure 4. Adsorbed configurations of propane-1,3-diphosphonate on the flat surfaces of barium sulfate.

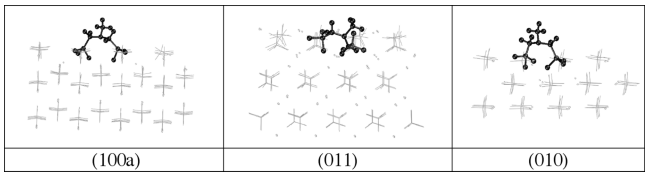

Figure 5. Adsorbed configurations of MNDP on barium sulfate. The three lowest replacement energies were found on the (100a), (011), and (010) faces.

adsorbed onto the surface. It can be seen from these new results that the stronger interatomic potential favors lattice matching and on most faces this results in both phosphonate groups being "adsorbed". The only exception is the (101) face where adsorption of only one phosphonate group is favored, due to the internal strain, and in order to conform to the space available.

Apart from the newer, lower surface energies calculated for the (001) and (210) surfaces, the different ordering of the results in comparison with previous literature could be attributed to computational restraints and the method used, which fixed the surface prior to minimizing the whole system. In addition to this method, we evaluated others such as simultaneous surface and organic relaxation. However, the different results are also due to the more attractive $Ba-O_{phos}$ interatomic potential as noted above, which has changed the lattice-matching component in such a way that it becomes more important than previously calculated. This shifts the balance between lattice matching and strain within the molecule more toward lattice matching. Despite these differences, both the current study and ref 16 show that the most favorable faces for adsorption are the (100a), (011), and (010) faces.

Turning to the MNDP molecule, we find that the replacement energies are in the following order:

(100a) > (011) > (010) > (101) > (211) > (001) > 210 > (100b)

The three lowest replacement energy configurations for this system can be seen in Figure 5. Interestingly, they are the same three faces on which the propane-1,3-diphosphonate molecule has the lowest replacement energy. Clearly, the modeling on this molecule (MNDP) suggests that the phosphonate groups replace the sulfate positions as best they can, although on the (011) face one phosphonate group is not as precisely aligned as it could be. Thus, the internal strain on the molecule has a significant contribution on this face. The main difference in

SCHEME 1: Schematic Showing How the Morphology of Rhombohedral Barite Crystals Is Altered in the Presence of MNDP, Which Is Assumed by ref 37 to Act on the (011) and (010) Faces

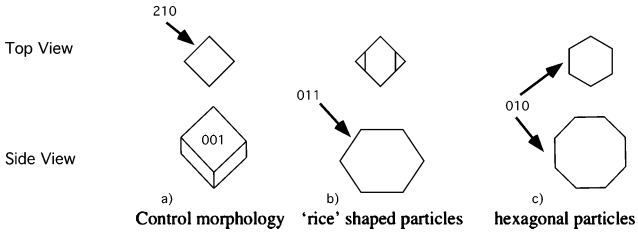

replacement energy ordering between MNDP and the previous diphosphonate are the replacement energy for the (101) face, which is more favorable, while the (210) and (100b) replacement energies are less favored. The possible causes for this difference in ordering are the presence of the methyl group (which does not have a very favorable interaction with the surface) and the presence of the nitrogen atom changing the central bonding geometry from tetrahedral to pyramidal (which would change the strain energy required to conform to the available space). Both of these factors could lead to changes in the MNDP configuration compared to the propane-1-diphosphonate such that the phosphonate distances are different and, therefore, different faces would be preferred. Also worth noting is that the more negative solvation energy for MNDP suggests a less surface-active molecule than the propane diphosphonate, and this is reflected in the smaller, more positive replacement energies for MNDP.

MNDP has been the subject of previous experimental work,[39] which showed that this additive alters the barium sulfate rhombs into "rice"-shaped particles. It was postulated that the phosphonate initially caused the appearance of (011) faces, followed by (010) faces to produce hexagonal particles. Scheme 1 shows the proposed morphology changes induced by MNDP on barium sulfate in accordance with the particle descriptions given in ref 39. We suggest that the "hexagonal" morphology is more accurately described as rounded and as such the (010) faces would be difficult to properly assign. However, given the ordering of replacement energies, it is tempting to suggest that if new faces were to emerge, they would indeed be the (011) and (010) faces. One problem, however, was that no interaction of MNDP with the (100a) barite surface was observed experimentally. To test this further, the effect of MNDP was investigated at much higher additive concentrations and at relatively high pH (in order to be certain the phosphonate groups were deprotonated). The results, presented in Figure 6b, show that at 0.23 mM MNDP the barium sulfate particles are still quite rounded and are reminiscent still of the rice-shaped particles, while at the higher concentration of 0.46 mM the barium sulfate particles are significantly flattened (Figure 6c). Selected area electron diffraction (SAED) in the TEM (Figure 6d) showed that the basal plane of these particles is most likely the (010) one. Thus, at higher concentrations, the less energetically favored faces start to be affected. However, the expected interaction with the (100a) face was not observed.

For NTMP, we find the following order of replacement energies (see Figure 7 for the three lowest replacement energy configurations):

$$(100a) > (011) > (101) > (211) > (010) > (100b) > (001) > (210)$$

For the configurations given in Figure 7, the replacement energy is generally lowest when the phosphonate groups replace

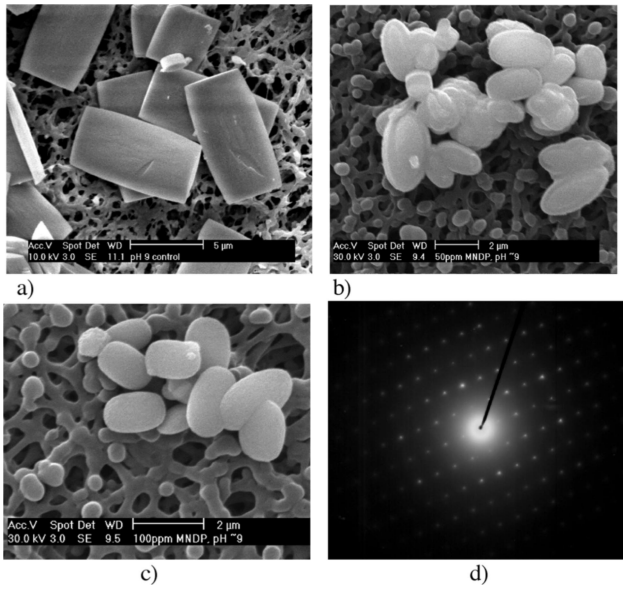

Figure 6. SEM photographs of barium sulfate particles precipitated in the presence of MNDP at pH 9: (a) control (no MNDP); (b) 0.23 mM MNDP; (c) 0.46 mM MNDP (the porous background is due to filter paper); (d) SAED of particles formed in the presence of 0.46 mM MNDP.

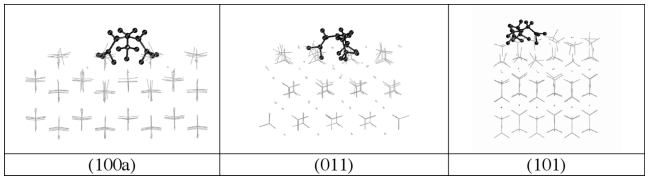

Figure 7. Adsorbed configuration of NTMP on barium sulfate: the three lowest replacement energy configurations.

the sulfate groups and try to match the lattice positions of the sulfate molecules. Clearly, this is achieved on the (011) and (100a) faces but not so well on the (101) face. The backbone of the NTMP sits slightly above the surface for all of the faces, suggesting once again that the CH_2 backbone does not interact favorably with the surface.

NTMP has recently been investigated using molecular modeling on barite for both flat terraces and kink sites,[19] but this study is not directly comparable with our own, first because it involved investigation of only the (001) face, second, it involved adsorption of only two of the three NTMP phosphonate groups, and finally, no adsorption configurations were given.

From conductivity studies,[8,9,25] we have observed similar morphological effects of NTMP on the precipitation of barium sulfate as ref 39; in this paper, it was suggested that the particles formed at relatively high concentrations of NTMP were (001) disks. Like the MNDP molecule, the NTMP additive is calculated to have a strong interaction on the (011) face, which was observed in our barite particles (see Figure 8) by their rounding. From our results, it appears that the disk could also be the (100) face (see Scheme 2). In terms of replacement energy, both the (001) and (100b) faces are energetically unfavorable, so if these were indeed (100) disks, they should be due to the interaction with the (100a) face.

To resolve this, particles formed in the presence of NTMP at a concentration that would produce disks (i.e., as in Figure 8c) were examined by TEM. The disk-shaped particles were found to be single crystals (Figure 9a and b), and sharp selected area electron diffraction (SAED) patterns were obtained from thin regions near the edge of the disks. Indexing of the SAED

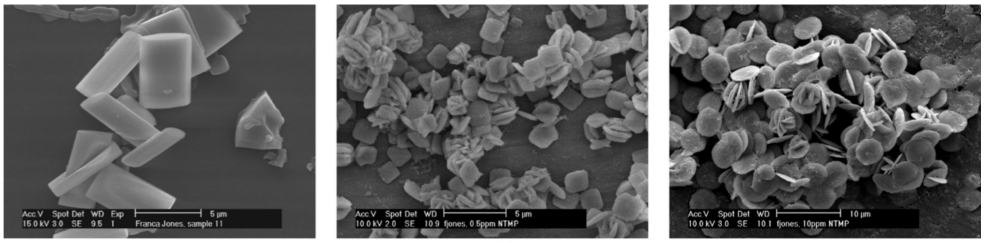

Figure 8. Barium sulfate particles formed in the presence of an increasing concentration of NTMP: (a) 0 mM NTMP; (b) 0.002 mM NTMP; (c) 0.037 mM NTMP.

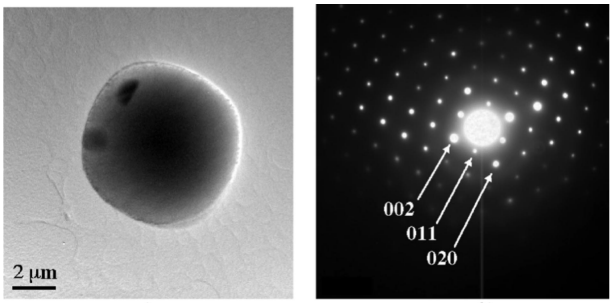

Figure 9. (a) TEM image of a barium sulfate particle formed in the presence of 0.037 mM NTMP and (b) SAED pattern obtained at the edge of this particle.

patterns demonstrates that the "flat" face of the disk corresponds to the (100) plane. It is clear from this that the flat face is not the (001) face but is the (100) face, as predicted by the molecular modeling simulations. However, it seems that higher concentrations tend to be required in order for less energetically favored faces to be observed, as for MNDP. Reasons for the differences in the predicted and observed interactions are given in the Discussion section.

For EDTP, the replacement energies follow the order

$$(100a) > (100b) > (001) \approx (210) > (101) > (010) > (011) > (211)$$

the four lowest configurations of which are shown in Figure 10.

It is clear from this that EDTP is able to interact favorably on all four of these faces, as it can match the sulfate lattice positions extremely well. The structure of the surface layer is only slightly perturbed by the presence of such a "large" organic molecule. Also, it is remarkable how similar the configurations are of EDTP in the (100a) and (001) surfaces, with the EDTP molecule essentially adopting the same tetrapodal position. The backbone lies slightly above all of the surfaces.

Comparison with experimental morphologies[8,9] shows that all of the predicted faces are stabilized with respect to the control particles[40] (Figure 11). As shown in Scheme 2, the control particles are pillow shaped, with the ends being the (001) faces and the rounded faces being (*hk*0) faces (Figure 11a). At low concentrations of EDTP (Figure 11b), the (001) face becomes the dominant basal face, with the side faces being the (210) and (100) faces; this gives the particles an elongated hexagonal

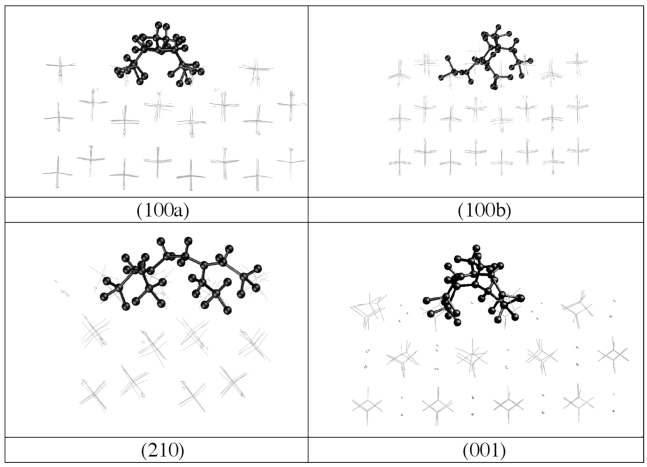

Figure 10. Adsorbed configuration of EDTP on barium sulfate: the four lowest replacement energy configurations.

appearance when viewed down the (001) face. At higher EDTP concentrations (Figure 11c), long bundles of fiberlike barium sulfate particles starting from a point are formed. As with other polymer phosphonates which have been found to produce barium sulfate fibers, a strong interaction with either the (210), (001), or (211) face is suggested[41] from TEM analysis, an observation which correlates well with our replacement energy results.

The barium ions on the surface interact strongly with the phosphonate molecule. In Figure 12, the phosphonate to barium ion interaction is shown in greater detail for the most energetically favorable configuration on the (100a) face. From the top view (Figure 12a), it is not immediately obvious that most phosphonate oxygen atoms have interactions with two barium ions. It is found that there are, in fact, 21 barium ion to oxygen (on the additive) atom distances less than 3 Å. A slightly off-center picture in Figure 12b shows how the oxygen atoms bind with two barium ions for one of the four phosphonate groups. The oxygen atom (on the phosphonate groups) to barium ion distance on the (100a) face varies from 2.2 to 2.9 Å, with the average distance being ~2.3 Å.

Discussion

It is important to recognize that crystal growth and inhibition is a complex process that alters with supersaturation and can differ from one crystal face to another. This is true for barium

SCHEME 2: Barium Sulfate Disks Could Have (100) Basal Faces as Opposed to (001) Faces

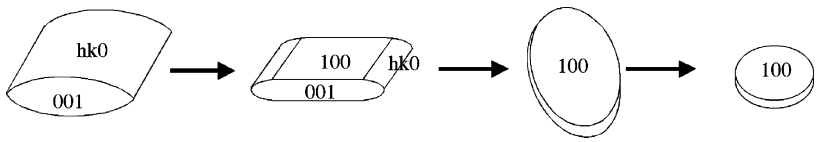

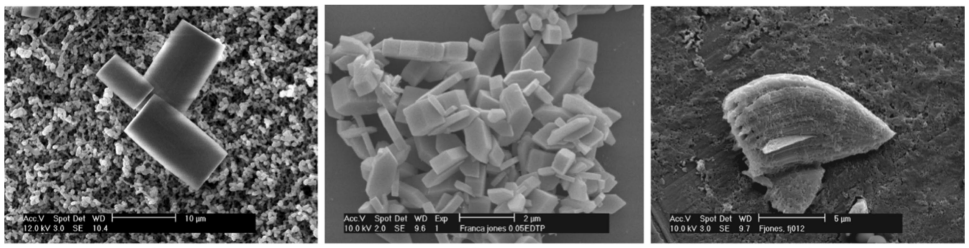

Figure 11. SEM micrograph of barium sulfate: (a) control particle; (b) obtained in the presence of 0.00012 mM EDTP; (c) obtained in the presence of 0.0012 mM EDTP.

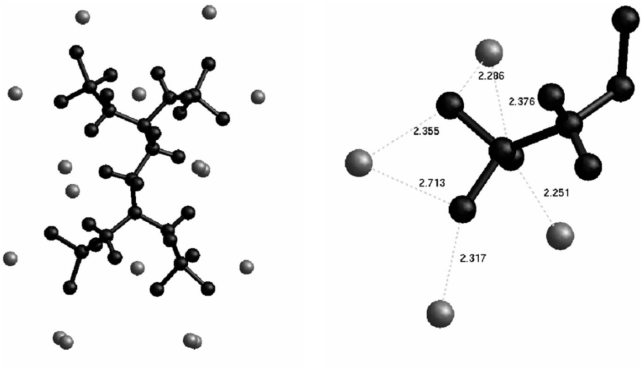

Figure 12. Phosphonate interaction with barium ions from the lowest replacement energy configuration of EDTP on the barium sulfate (100a) surface: (a) the adsorbed EDTP molecule (black) as viewed down the (001) with the sulfate molecules removed so that the barium ions (grey) are visible; (b) a staggered view of how the oxygen atoms on the EDTP molecule interact with barium ions (grey) on the (100a) surface.

sulfate. Previous work has shown that the (001) face grows on screw dislocations via spiral growth at low supersaturations and by 2D nucleation of islands at higher supersaturations. In contrast, the (210) face grows by 1D growth.[42] Thus, a more accurate way of determining the effect on crystal growth would be to take into consideration these modes of growth at the relevant supersaturation. Obviously, the work presented here is the first part of a major undertaking to model this system appropriately. In all of these systems, however, adsorption of an additive occurs, and in this work, we begin by understanding the adsorption of these additives on flat surfaces (terraces).

An additional point to be made is that a periodic system necessitates a neutral cell; otherwise, infinite surface charges result, making the system unstable. However, while sulfate vacancies are created to compensate for the charged additive, this does not force the adsorption of the functional groups into those vacancies. Thus, if adsorption of one phosphonate is preferred over two, then this should be observed in the modeling. The use of such a periodic system is well accepted, as can be seen in the literature already discussed.[10,12−18,42]

Tabulating the four most negative replacement energies for all of the molecules studied, we find that the faces with the preference for adsorption are as follows:

propane-1,3-diphosphonate	(100a) > (011) > (010) > (211) > (210)
MNDP	(100a) > (011) > (010) > (101) > (211)
NTMP	(100a) > (011) > (101) > (211) > (010)
EDTP	(100a) > (100b) > (210) ≈ (001) > (101)

These results shows that in all cases the phosphonate groups basically interact strongly with the same small number of surfaces. In particular, all adsorb favorably on the (100a) face. For molecules containing up to three phosphonate groups, the (011) face appears to consistently provide the next lowest replacement energy. The (101), (211), (210), (001), and (010) faces are sometimes favored and sometimes not, and the (100b) face seems to be among the least favored, except when EDTP is present. If growth of the (100) face were by half slices (as suggested by ref 37), then only every second growth layer would have the (100a) form. EDTP, which has a favorable interaction with both (100) faces, would be able to inhibit both forms, and the effect on the (100) face could then be observable even at low concentrations (as is seen in Figure 11). From TEM analysis of the particles formed, the interaction with the (100a) faces appears to be real for the NTMP case but requires higher concentrations. For MNDP, however, the results show that higher concentrations are required to observe effects on the less favored faces as the results showed the (010) interaction. Previous modeling[16] has also found the (100a) replacement energy to be favorable, but this was discounted on the basis that the (100a) face was not a low energy face and was not expected to form. The difference between the unrelaxed faces in that work was small, as previously discussed, and in this work, both faces were found to be low in energy depending on whether the surface energy or attachment energy criterion was used. We feel, therefore, that this face is worthy of being investigated and that the interaction with the (100a) face is real. However, it may be a less energetically favored face if adsorption does not take place on terraces but on step and kinks sites as discussed below.

Several points can be made here as to why there are some small differences between the predicted faces and the observed faces on which adsorption should be preferred:

1. This study does not take into account the speciation of the molecule but rather assumes all molecules are fully deprotonated. Thus, it is assumed that all of the phosphonate groups within the molecule interact with the surface, which may not be the case.

2. It does not model the zwitterionic character of the aminophosphonates. Thus, any hydrogen bonding between the N−H group and the surface is excluded.

3. We have modeled adsorption only on flat surfaces. Recent work has suggested that perhaps adsorption onto growth features (such as steps, kinks, and spirals) is more important than adsorption onto terraced surfaces for the obvious reason that precipitation normally occurs at such growth features.[42−44] While it is known that barium sulfate can grow by a "birth and spread" mechanism even at relatively low concentrations,[45] we should not exclude the possibility that even in the birth and spread regime, adsorption at steps and kinks is more important than adsorption onto flat surfaces. This may slightly alter the ordering of the faces with respect to their interaction with the organics as found in ref 19, and this in turn may explain why the effect on the (100) face is not always observed (if it were not the

TABLE 6: Replacement Energies (kJ mol^{-1}) for the Phosphonate Containing Molecules versus the Face on Which They Are Adsorbed on a Per-Phosphonate Group Basis (Solvation Energy Taken into Account)

face	propane-1,3-diphosphonate	MNDP	NTMP	EDTP
(001)	−403.18	−305.26	−337.3	−519.3
(210)	−390.5	−266.6	−330.7	−519.3
(211)	−404.8	−307.5	−394.9	−445.5
(010)	−439.4	−343.2	−383.1	−497.4
(011)	−492.9	−409.1	−455.0	−476.5
(101)	−375.6	−337.0	−418.7	−517.9
(100b)	−383.5	−230.1	−345.9	−549.1
(100a)	−533.5	−460.6	−495.6	−601.3

TABLE 7: Inhibition (%) of Barium Sulfate De-supersaturation for Various Concentrations (mM) of MNDP, NTMP, and EDTP

	inhibition (%)		
concentration (mM)	MNDP	NTMP	EDTP
0.0001			45.8
0.002	0.3		100
0.007		35.9	
0.016		50.3	
0.02	12.3		

most favored face for adsorption but only the second or third favored face).

4. This study only takes the solvent into consideration by way of solvation energies and does not explicitly take into consideration the fact that the surfaces may be hydrated to some degree. This could also alter the interaction of the organic molecules with various faces.

The more negative solvation energy resulted in the MNDP having a more positive replacement energy. The molecular modeling therefore predicts that the MNDP molecule would be a slightly worse inhibitor than the propane-1,3-diphosphonate molecule. More importantly, it is clear that as the number of phosphonate groups increases the replacement energy decreases (Table 5). This means that the greater the number of phosphonate groups, the more adsorption will be favored.

Perhaps more surprisingly, even on a per-phosphonate group basis, the larger EDTP molecule has a slightly more favorable replacement energy, as shown in Table 6. This is probably due to the fact that this molecule can rearrange to suit the available space with less internal strain than the smaller molecules and is shown by the more negative values over most faces (ranging from about −440 to −600 kJ mol^{-1}). The other three molecules show similar replacement energies, the majority of which range from ∼ −300 to ∼ −500kJ mol^{-1}. For these molecules, the differences lie with the most and least energetically favored faces. It perhaps suggests that the EDTP has just the right configuration and phosphonate distances to minimize the internal strain component. Table 7 shows the percent inhibition (defined as {1 − rate with additive present/rate of control} × 100) for the various additives investigated in this work. It is clear that even if we were to take into account the number of phosphonate groups present on each additive, the EDTP would still far outperform the others in terms of inhibition (as modeling predicts). If we assumed a linear trend with inhibition and divided by the number of phosphonate groups, the NTMP at 0.0002 mM (on a per-phosphonate group basis) would inhibit to the same degree as the MNDP at 0.01 mM on a per phosphonate group basis. The modeling results in Table 6 suggest that the MNDP and NTMP should be equivalent inhibitors (if the replacement energy on a per-phosphonate group basis is considered). However, this is not observed experimentally; as stated above, NTMP is a far stronger inhibitor even when the number of phosphonate groups is considered. It should be remembered that the model assumes completely deprotonated additives, and this is unlikely for MNDP at pH 6.[25] Thus, one reason the replacement energy on a per-phosphonate group basis does not correspond to the experimental trend could be the experimental procedure itself. Another reason is that adsorption on terraces may not be the preferred adsorption site and adsorption at steps and kinks may be more energetically favored. This could, in turn, change not only the preferred faces for adsorption but also the replacement energy values. The modeling of these molecules has been performed with one additive per cell, but each cell is slightly different in surface area, and due to charge differences, the surfaces can "accommodate" more molecules of lesser charge. As a guide, on the (001) face, the current model would represent an additive molecule coverage of ∼15−25% of a full monolayer.

The most significant interaction found in this work is the interatomic interaction between the barium surface ions and the oxygen atoms on the phosphonate molecules. Due to this, lattice matching (or molecular recognition) becomes more important in determining the replacement energy compared to the previous study.[16] In most configurations, each oxygen atom is in a position that maximized the number of barium ions with which it could interact and, not surprisingly, this generally coincides with a sulfate position in the barite lattice.

One would hope that there might be a direct link between the value of the replacement energy and the degree of inhibition, and indeed, conductivity experiments measuring the de-supersaturation rate show that, for the series MNDP, NTMP, and EDTP, where the number of phosphonate groups is increasing, the degree of inhibition also increases.[8,9] This matches the trends observed with the replacement energy (Table 5), so we can say that our potentials are accurately describing these systems overall.

Conclusions

Simulations of the adsorption of phosphonate molecules onto flat barium sulfate surfaces have been conducted using empirically derived potentials. These phosphonates appear to have a strong interaction with the (100a) and (011) barite surfaces. The replacement energy was always negative, suggesting that adsorption of the deprotonated molecules onto barium sulfate surfaces is energetically favorable. The replacement energy becomes more negative as more phosphonate groups are able to interact. Thus, if the molecules were fully deprotonated, the more phosphonate groups present, the more likely adsorption onto the surface is.

The premise that additives are effective inhibitors of barium sulfate precipitation when they can match lattice positions is generally borne out by the results of this study. Lattice matching of the sulfate position appears to be dominant in determining the replacement energy. This can be understood in terms of maximizing the additive's interaction with surface barium ions. Internal strain from the organic additive trying to lattice match is also important, and our results suggest that the smaller the molecule, the more important this effect will be. Small molecules do not have the same degrees of freedom as larger molecules to orient themselves to a particular space.

The success of using molecular modeling to predict the relative strength of these molecules' inhibition of barium sulfate precipitation has been demonstrated. Furthermore, for the first time, the predicted interaction of the additives with the (100a) face has been demonstrated experimentally for two of the

organic additives (NTMP and EDTP). However, for NTMP, high concentrations were required to observe any effect on the (100) face. This observation could be due either to the modeling being conducted on terraces rather than kinks or steps or to the effects of solvent and/or the growth mechanism of the (100) surface. Future work will focus on refining the model and to studying the effects on growth features rather than on flat surfaces to extend the predictive value of our system.

Acknowledgment. We gratefully acknowledge that this research has been supported under the Australian Government's Cooperative Research Centre (CRC) Program, through the AJ Parker CRC for Hydrometallurgy.

Supporting Information Available: Tables showing the empirical constants and potential types required for the molecular mechanics calculations. All cutoffs were set at 15 Å except for the Ba−O Buckingham potential set at 10 Å. This material is available free of charge via the Internet at http://pubs.acs.org.

References and Notes

(1) Schwarzer, H.-C.; Peukert, W. *Chem. Eng. Technol.* **2002**, *25* (6), 657.

(2) Sorbie, K. S.; Mackay, E. J. *J. Pet. Sci. Eng.* **2000**, *27*, 85.

(3) Breen, P. J.; Downs, H. H.; Diel, B. N. *R. Soc. Chem. (Spec. Publ.)* **1991**, *97*, 186.

(4) Benton, W. J.; Collins, I. R.; Grimsey, I. M.; Parkinson, G. M.; Rodger, S. A. *Faraday Discuss.* **1993**, *95*, 281.

(5) Amjad, Z. *Water Treat.* **1994**, *9*, 47.

(6) Graham, G. M.; Boak, L. S.; Sorbie, K. S. Presented at the International Symposium on Oilfield Chemistry, Society of Petroleum Engineers, 1997; Paper SPE37273.

(7) Davey, R. J.; Black, S. N.; Bromley, L. A.; Cottier, D.; Dobbs, B.; Rout, J. E. *Nature* **1991**, *353*, 549.

(8) Jones, F.; Stanley, A.; Oliveira, A.; Rohl, A. L.; Reyhani, M. M.; Parkinson, G. M.; Ogden, M. I. *J. Cryst. Growth* **2003**, *249*, 584.

(9) Jones, F.; Oliveira, A.; Rohl, A. L.; Reyhani, M. M.; Parkinson, G. M.; Ogden, M. I. *J. Cryst. Growth* **2002**, *237*−*239*, 424.

(10) Allan, N. L.; Rohl, A. L.; Gay, D. H.; Catlow, C. R. A.; Davey, R. J.; Mackrodt, W. C. *J. Chem. Soc., Faraday Discuss.* **1993**, *95*, 273.

(11) Jang, Y. H.; Chang, X. Y.; Blanco, M.; Hwang, S.; Tang, Y.; Shuler, P.; Goddard, W. A., III. *J. Phys. Chem. B* **2002**, *106*, 9951.

(12) de Leeuw, N. H. *J. Phys. Chem. B* **2002**, *106*, 5241.

(13) de Leeuw, N. H.; Cooper, T. G. *Cryst. Growth Des.* **2004**, *4* (1), 123.

(14) Jones, F.; Rohl, A. L.; Farrow, J. B.; van Bronswijk, W. *Phys. Chem. Chem. Phys.* **2000**, *2*, 3209.

(15) (a) Fogg, A. M.; Freij, A. J.; Rohl, A. L.; Ogden, M. I.; Parkinson, G. M. *J. Phys. Chem. B* **2002**, *106*, 5820. (b) Fogg, A. M.; Freij, A. J.; Oliveira, A.; Rohl, A. L.; Ogden, M. I.; Parkinson, G. M. *J. Cryst. Growth* **2002**, *234*, 255.

(16) Rohl, A. L.; Gay, D. H.; Davey, R. J.; Catlow, C. R. A. *J. Am. Chem. Soc.* **1996**, *118*, 642.

(17) Coveney, P. V.; Davey, R. J.; Griffin, J. L. W.; He, Y.; Hamlin, J. D.; Stacckhouse, S.; Whiting, A. *J. Am. Chem. Soc.* **2000**, *122*, 11557.

(18) Bromley, L. A.; Cottier, D.; Davey, R. J.; Dobbs, B.; Smith, S.; Heywood, B. R. *Langmuir* **1993**, *9*, 3594.

(19) Pina, C. M.; Putnis, C. V.; Becker, U.; Biswas, S.; Carroll, E. C.; Bosbach, D.; Putnis, A. *Surf. Sci.* **2004**, *553*, 61.

(20) Gale, J. D.; Rohl, A. L. *Mol. Simul.* **2003**, *29* (5), 291.

(21) Gay, D. H.; Rohl, A. L. *J. Chem. Soc., Faraday Trans.* **1995**, *91* (5), 925.

(22) Wulff, G. *Z. Krystallogr.* **1901**, *34*, 449.

(23) Fleming, S. D.; Rohl, A. L. *Z. Kristallogr.* **2005**, *220* (5, 6), 580.

(24) Westerback, S.; Rajan, K. S.; Martell, A. E. *Nature* **1956**, *178*, 321.

(25) Jones, F.; Stanley, A.; Oliveira, A.; Rohl, A. L.; Reyhani, M. M.; Parkinson, G. M.; Ogden, M. I. *J. Cryst. Growth* **2003**, *249*, 584.

(26) Jones, F.; Rohl, A. L.; Ogden, M. I.; Parkinson, G. M. Scale formation and inhibition. Presented at the 16th International Symposium on Industrial Crystallization, Dresden, Germany, Sept 2005 (conference proceedings published on CD-ROM).

(27) Wilson, M. P. Personal communication, 2002.

(28) *InsightII*, version 2.3.6; Biosym Technologies Inc.: San Diego, CA, 1995.

(29) Hehre, W. J.; Yu, J.; Klunzinger, P. E. Wavefunction, Inc.: Irvine, CA, 1997.

(30) Stewart, J. J. P. *J. Comput. Chem.* **1989**, *10*, 221.

(31) Shi, S.; Yan, L.; Yang, Y.; Fisher-Shaulsky, J.; Thacher, T. *J. Comput. Chem.* **2002**, *24* (9), 1059.

(32) Colville, A. A.; Staudhammer, K. *Am. Mineral.* **1957**, *52*, 1877.

(33) Hawthorn, F. C.; Ferguson, R. B. *Can. Mineral.* **1975**, *13*, 181.

(34) Haussühl, S. *Z. Kristallogr.* **1990**, *192*, 137.

(35) Dove, P. M.; Czank, C. A. *Geochim. Cosmochim. Acta* **1995**, *59*, 1907.

(36) Hill, R. J. *J. Can. Mineral.* **1977**, *15*, 522.

(37) Hartman, P.; Heijnen, W. M. M. *J. Cryst. Growth* **1983**, *63*, 261.

(38) Archibald, D. D.; Gaber, B. P.; Hopwood, J. D.; Mann, S.; Boland, T. *J. Cryst. Growth* **1997**, *172*, 231.

(39) Black, S. N.; Bromley, L. A.; Cottier, D.; Davey, R. J.; Dobbs, B.; Rout, J. E. *J. Chem. Soc., Faraday Trans.* **1991**, *87*, 3409.

(40) Jones, F.; Rohl, A. L. *Mol. Simul.* **2005**, *31* (6, 7), 393.

(41) Qi, L.; Cölfen, H.; Antonietti, M. *Angew. Chem., Int. Ed.* **2000**, *39* (3), 604.

(42) Becker, U.; Risthaus, P.; Bosbach, D.; Punits, A. *Mol. Simul.* **2002**, *28* (6, 7), 607.

(43) Nygren, M. A.; Gay, D. H.; Catlow, C. R. A.; Wilson, M. P.; Rohl, A. L. *J. Chem. Soc., Faraday Trans.* **1998**, *94*, 3685.

(44) Davis, K. J.; Dove, P. M.; De Yoreo, J. J. *Science* **2000**, *290*, 1134.

(45) Pina, C. M.; Becker, U.; Risthaus, P.; Bosbach, D.; Putnis, A. *Nature* **1998**, *395* (6701), 483.